Available online at www.sciencedirect.com
SCIENCE DIRECT®
Coordination Chemistry Reviews 248 (2004) 1407–1420
COORDINATION CHEMISTRY REVIEWS
www.elsevier.com/locate/ccr

Review

# Resonance micro-Raman spectrophotoelectrochemistry on nanocrystalline $TiO_2$ thin film electrodes sensitized by Ru(II) complexes

Thomas Stergiopoulos [a], Marie-Claude Bernard [b], Anne Hugot-Le Goff [b], Polycarpos Falaras [a,*]

[a] *Institute of Physical Chemistry, NCSR "Demokritos", 153 10 Aghia Paraskevi Attikis, Athens, Greece*
[b] *UPR 15 du CNRS "Laboratoire des Interfaces et Systèmes Electrochimiques", Université Pierre et Marie Curie, 75252 Paris, Cedex 05, France*

Received 9 October 2003; accepted 29 March 2004
Available online 2 June 2004

## Contents



## Abstract

Resonance micro-Raman spectrophotoelectrochemistry combines spatial resolution, offering the ability to detect the vibration properties of separate components in the dye nanocrystalline cell, with a dynamic control of the electrochemical interface via the applied potential. This enables us to obtain new insights in the mechanism of photosensitization of large band-gap semiconductors, elucidate the interactions between the semiconductor, dye and redox couple, detect the creation of new species and/or the existence of parasite reactions and finally permit the optimization of the cell's performance. Our group was the first to study the dye chemisorption on nanocrystalline titanium dioxide thin films using resonance micro-Raman spectroscopy. The investigation was extended to polarized dye-sensitized working photoelectrodes aiming at elucidating the vibrational properties of the dye, especially in the aromatic region as well as those of the iodides in the range of the oxide vibration bands. Recent investigations revealed the presence of new vibration bands in the low wave number region, mainly at 112 and 167 $cm^{-1}$ and the dependence of their intensity on the applied potential. In the present work, we confirm the general character of the phenomenon by using a number of dyes with a variety of ligands. The vibrational properties of sensitized electrodes and corresponding cells realized with dyes recently synthesized (containing $PPh_3$, bdmpp, dc-bpy, iph-terpy, phpa-terpy, $Cl^-$, and $NCS^-$ ligands) are compared with photoelectrodes and cells using commercial dyes (N3 and black-dye). We examine the influence of the dye, the redox couple, the electrolyte, the titania preparation technique

*Abbreviations:* dc-bpy, 2,2′-bipyrine-4,4'-dicarboxylic acid; tc-terpy, 2,2′:6′,2″-terpyridine-4,4′,4″-tricarboxylic acid; $PPh_3$, triphenyl phosphine; bdmpp, 2,6-bis(3,5-dimethyl-*N*-pyrazoyl) pyridine; iph-terpy, 2,2′:6′,2″-terpyridine-4-(4‴-iodophenyl); phpa-terpy, 2,2′:6′,2″-terpyridine-4-(4‴-phenyl phosphonic acid)

* Corresponding author. Tel.: +30-210-6503644; fax: +30-210-6511766.
*E-mail address:* papi@chem.demokritos.gr (P. Falaras).


doi:10.1016/j.ccr.2004.03.023

and the laser excitation line on the presence of these bands as well as on their behavior under anodic and cathodic bias. The nature of these bands is discussed on the basis of the sensitization mechanism and this allows their attribution to new species formed during the cell's operation.


*Keywords:* Raman spectrophotoelectrochemistry; Ru-dyes; Triiodide; Solar cells

## 1. Introduction

Grätzel and co-workers [1,2], 12 years ago, discovered that dye-sensitized nanocrystalline solar cells (DSSC) could convert visible light to electricity with efficiency as high as 10%. The development of these systems was based on the preparation of rough, high surface area titanium dioxide thin film electrodes, the synthesis of transition metal complexes presenting strong and broad metal to ligand charge transfer (MLCT) absorption bands in the visible part of the solar spectrum acting as efficient light capturing antennas, as well as the use of a redox couple in an appropriate medium [3]. In such a device, the dye is chemically adsorbed via an ester-like linkage on the semiconductor surface in the form of a monolayer. Following visible light absorption, the dye is excited by electron transfer from the highest occupied molecular orbital (HOMO) orbital belonging to the Ru metal to the LUMO orbital concentrated on one ligand. Photoexcitation is followed by very fast electron injection (in the femto second range) into the $TiO_2$ conduction band through the semiconductor–dye connection. A redox couple in the electrolyte is used for regenerating the oxidized form of the adsorbed dye, acting as a charge mediator between the photoelectrode and the counter electrode [4].

The sensitization mechanism is well established, but there is a lack of direct information indicative of interactions between the redox couple and the sensitizer. The iodide/triiodide ($I^-/I_3^-$) system is the most widely used redox couple in both aqueous and non-aqueous media. Although a great number of papers have been published in the field, many of them concern the photosensitization mechanism, but only a few reports deal with the $I^-/I_3^-$ couple [5–7]. Optimization of the cell performance requires a continuous harmonic operation and excellent compatibility between its different elements (the redox couple included) as well as complete elucidation of the reactions taking place near the photoelectrode.

Further development and practical issue on dye-sensitized solar cells require new analytical tools giving information on the photoelectrode–electrolyte interface. Resonance Raman spectroscopy has an ample temporal and spatial resolution to probe the vibrational properties of separate components (by using the Raman microscope, one can focus on the semiconductor, dye, or the electrolyte alternatively and the corresponding interfaces) during the operation of the DSSC device. Our group was the first to study the dye chemisorption on nanocrystalline titanium dioxide thin films using resonance micro-Raman spectroscopy [8,9]. The investigation was recently extended to polarized dye-sensitized working photoelectrodes aiming at elucidating the dye–redox couple interactions by studying the vibration properties of the dye, especially in the aromatic region as well as in the range of the oxide vibration bands [10]. Raman experiments on sensitized photoelectrodes under real photocurrent conditions revealed the presence of new vibration bands in the low wave number region, mainly at 112 and 167 $cm^{-1}$ and confirmed the dependence of their intensity on the applied potential. The first band was attributed to triiodide and the second to dye–redox couple interaction (formation of "DI" species) [11–13].

However, some questions arise on the presence and the behavior of the lines at 112 and 167 $cm^{-1}$: are they still present when the iodide/triiodide redox couple is replaced by another electron donor (i.e. hydroquinone), do we expect a similar behavior in aqueous systems or organic media (i.e. propylene carbonate), what is the effect of the polarization potential; is there any dependence on the titania substrate or the laser wavelength, may we attribute the 167 $cm^{-1}$ Raman band to NCS/$I_2$ or to electrolyte/$I_2$ complex formation [15,16], and finally: what happens with other dyes that do not contain the thiocyanato ligand?

Vibrational spectrophotoelectrochemistry permits a dynamic Raman investigation and the follow-up of the sensitization mechanism. The investigation of the photoelectrode/electrolyte interface is possible by direct observation of the intensity variation of the main vibration bands differentiated by the applied potential (positive or negative). In the present work, we confirm the general character of the phenomenon by using a number of dyes with a variety of ligands. We examine the influence of the dye, the redox couple, the electrolyte, the titania preparation technique and the laser excitation line on the presence of these bands as well as on their behavior under anodic and cathodic bias. The nature of these bands is discussed on the basis of the sensitization mechanism and this allows their attribution to the iodide/dye interaction and to the formation of new species formed during the cell's operation.

## 2. The choice of the dyes

The dye is the heart of the titania nanocrystalline solar cell. It has to accomplish a multifunctional role including a number of different tasks: absorb the incident light; inject electrons into the semiconductor conduction band; react with the redox couple in order to be regenerated; block the $TiO_2$/electrolyte interface to reduce the dark current. As a result, the cell performance mainly depends on the choice of an efficient light capturing antenna, which usually con-

sists of a Ru(II) complex with nitrogen heterocyclic ligands (having delocalised π or aromatic ring system, i.e. diazo- or triazo-aromatic ligands and substituted analogues) bearing functional anchoring groups (to ensure monomolecular chemical attachment).

An extremely large number of complexes (several hundreds) have been synthesized so far and proved to successfully sensitize titanium dioxide. Ruthenium 535 (or N3) and ruthenium 620 (or "black-dye") are among the most efficient dye sensitizers. They are commercial products (Solaronix), they contain bipyridyl or terpyridyl ligands and their common characteristic is that they both contain the isothiocyanato ($NCS^-$) group. This ligand of low electronegativity is believed to participate with Ru to the HOMO and therefore it plays an important role in the complex stabilization and may facilitate the dye regeneration by the redox couple. It is therefore expected to orient our investigation on these dyes. On the other side, two new complexes of the type [Ru(bdmpp)(dc-bpy)X]($PF_6$) (where X = $Cl^-$, $NCS^-$) were recently synthesized and successfully tested as molecular antennas in nanocrystalline $TiO_2$ solar cells [17,18]. The first ligand, bdmpp [2,6-bis(3,5-dimethyl-*N*-pyrazoyl)pyridine] can be considered as a terpyridine derivative, exhibiting significantly different electronic properties. The complexes differ slightly, as in the second complex, $Cl^-$ is replaced by –N=C=S and the investigation of their vibration properties permits to test directly the validity of the thiocyanato ligand exchange mechanism. To check the possible influence and/or interference of the other ligands on vibration properties and especially to give emphasis on a possible role of the functional groups which ensure the linkage to $TiO_2$, two other complexes containing triphenyl phosphine and substituted terpyridine ligands were also examined.

The list of the different dyes with corresponding ligands used in the Raman study is presented in Table 1. Five of them bear carboxylic acid anchoring moieties whereas the sixth a phosphonic acid one. These groups can serve as interlocking agents (the adsorption through a phosphonate group is believed to offer a higher stability of the chemisorbed dye, especially in water and in a very broad pH range) [19,20]. The six dyes present the theoretical interest to contain a variety and combination of ligands and their co-existence is expected to differentiate the Raman spectra, leading to a better understanding of the dye–redox couple interaction.

## 3. Resonance Raman on dye–monolayers chemisorbed on $TiO_2$ electrodes

Rough, and fractal, high surface area nanostructured $TiO_2$ electrodes (5 μm in thickness) were prepared by doctor-blading the Degussa P25 titanium dioxide powder [21] on TEC 15 conductive glass substrates (Hartford Glass Co. Inc., fluorine-doped $SnO_2$ glass with a sheet resistance of 15 Ω per square). Detailed analysis of the morphological characteristics performed by AFM has shown that the doctor-blade $TiO_2$ films present a high degree of surface complexity, confirmed by a value of fractal dimension as high as 2.41. Surface modification of the titanium oxide was achieved following overnight immersion in $10^{-4}$ M alcoholic solution of the complexes [22]. Resonance Raman spectroscopy has successfully been used to characterize the grafting of the six Ru(II) dyes on the $TiO_2$ electrode surface. The Raman experiments were performed using two different apparatus: an ISA Jobin–Yvon–Horiba LABRAM Spectroscope with notch filter and excitation at 632.8 nm by He–Ne laser or 514.5 nm by Argon laser, and a Dilor Omars 89 system with a charge coupled device (CCD) detection and an Argon laser allowing the use of three different lines, 457.9, 488 and 514.5 nm.

The Raman spectra are able to offer structural information on the oxide and sensitizer as well as the relevant changes induced by the dye chemisorption on the semiconductor surface. Besides their great importance for efficient light harvesting, the existence of broad and intense MLCT bands is at the origin of the resonance Raman effect observed on nanocrystalline titania solar cells. In fact, the technique makes use of the excitation close to the MLCT absorption band maxima (Table 1) of the dye and this situation results in a charge transfer resonant contribution. The intensity of the corresponding vibration bands is significantly enhanced (high resonant effect in the dye) and this permits to detect the chemisorbed dye, present in the form of just a monolayer on the titania electrode surface.

The obtained spectra of the sensitized photoelectrodes, reported on Fig. 1a, contain information for both the sensitizers and the semiconductor substrate. The spectral features present in the 1300–1600 $cm^{-1}$ wave number region are the fingerprints of the chemisorbed dyes. The Raman vibration bands are broader than the corresponding bands of the dyes in the powder form or in solution (not shown here) and the most important of them are summarized in Table 2. Besides some differences in peak position and intensity, which permit to differentiate each sensitized electrode, they are typical of the pyridine ring and the major part of them is assigned to C–C or C–N main ring stretchings. Thus, very strong vibration bands centered at 1032 and 1260 $cm^{-1}$ (C–H bending) as well as at 1607, 1540, 1472 $cm^{-1}$ in the C–C stretching region were observed for Ru-Cl and Ru-NCS dyes. Nevertheless, a detailed analysis and attribution of the different Raman vibration bands in this range has been already made [10,11,20]. In addition, the spectral characteristics in the low wave numbers allows us to check the titania structural modification. Thus anatase at: 143 [$E_g$ (vs)], 196 [$E_g$ (vvw)] 396 [$B_{1g}$ (s)] 517 [$A_{1g}$, $B_{1g}$ (s)] $cm^{-1}$], 637 [$E_g$ (vs)] $cm^{-1}$ and also rutile at: 448 [$E_g$(w)], 616 [$A_{1g}$(w)] $cm^{-1}$ titania Raman vibration bands were observed. This is explained by the fact that the original material ($TiO_2$ Degussa P25) contains both phases (∼75% anatase and ∼25% rutile). Furthermore, the width of the strongest anatase $E_g$ Raman vibration band allows the estimation of the size of $TiO_2$ nanocrystallites at about 25 nm, a value very close to that obtained from the

Table 1
List of dyes with related ligands, corresponding MLCT maximum (nm) and molar extinction coefficient values (in parentheses) for the Ru(II) dyes used in the resonance Raman investigation

| Dye | Aromatic ligand | Molecular structure | MLCT maximum (nm) ε ($M\,cm)^{-1}$ |
|---|---|---|---|
| $Ru(dc\text{-}bpy)_2(NCS)_2$ (N3) | dc-bpy | 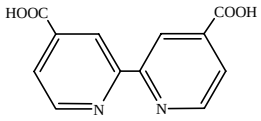 | 534 (14200) |
| $Ru(tc\text{-}terpy)(NCS)_3$ (black dye) | tc-terpy | 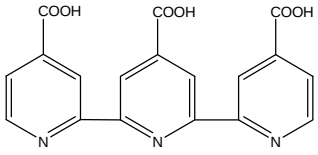 | 620 (6000) |
| $Ru(PPh_3)_2(dc\text{-}bpy)Cl_2$ ($Ru\text{-}PPh_3$) | $PPh_3$ | 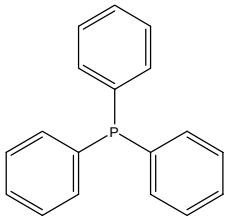 | 521 (3400) |
| $[Ru(bdmpp)(dc\text{-}bpy)Cl](PF_6)$ (Ru-Cl) | bdmpp | 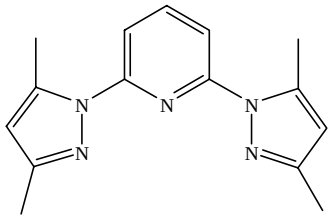 | 483 (21000) |
| $[Ru(bdmpp)(dc\text{-}bpy)(NCS)](PF_6)$ (Ru-NCS) | iph-terpy | 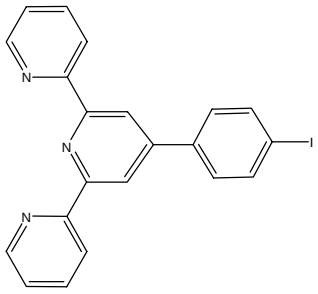 | 475 (23400) |
| $[Ru(iph\text{-}terpy)(phpa\text{-}terpy)Cl_2$ (Ru-terpy) | phpa-terpy | 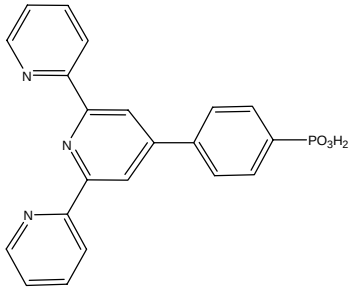 | 490 (22000) |

XRD patterns (estimated at 23 nm) or from the direct AFM analysis (measured at 20–25 nm). It must be mentioned that the use of different laser excitations results in differences of the Raman vibration bands, especially those associated with dyes. The use of the red laser at 632.8 nm significantly decreases the ensemble of the vibration bands between 1000 and 1600 $cm^{-1}$ (not shown). On the contrary, the titanium dioxide bands were not affected. This is an incontestable proof that we have to deal with a resonance Raman effect.

## 4. Raman investigation in aqueous electrolytes

### 4.1. Open circuit potential conditions

Spectacular changes on the Raman vibration properties occurred when the dye-coated titania photoelectrodes were immersed in an electrolytic solution containing the electron donor under open circuit potential (OCP) conditions. Fig. 1b presents the corresponding spectra obtained with the differ-

Table 2
Main vibration Raman bands for dye complexes chemisorbed on nanocrystalline $TiO_2$ (Degussa P25) thin film electrodes, ex situ

| Dye on $TiO_2$ | Raman vibration bands ($cm^{-1}$) |
|---|---|
| $Ru(dc\text{-}bpy)_2(NCS)_2$ (N3 dye) | 1610 (w), 1538 (vw), 1474 (s), 1385 (vw), 1263 (w), 1031 (s), 632 (vs), 511 (s), 389 (s), 193 (vvw), 139 (vvs) |
| $Ru(tc\text{-}terpy)(NCS)_3$ (Ru620 or black dye) | 1609 (s), 1537 (vs), 1445–14761 (s), 1280–1314 (w), 1020–1046 (w), 692 (w), 639 (s), 517 (s), 394(w), 309 (vw), 144 (vvs) |
| $Ru(PPh_3)_2(dc\text{-}bpy)Cl_2$ (Ru-$PPh_3$) | 1610 (s), 1540 (vs), 1476 (s), 1436 (w), 1368 (w), 1262 (s), 1035 (w), 637 (s), 516 (s), 398 (s), 199 vw), 148 (vvs) |
| $[Ru(bdmpp)(dc\text{-}bpy)Cl](PF_6)$ (Ru-Cl) | 1604 (w), 1541 ((w), 1478 (s), 1432 (vw), 1270 (s), 1031 (s), 773 (s), 700 (s), 634 (vs), 514 (s), 396 (vs), 369 (vs), 198 (vvw), 141 (vvs) |
| $[Ru(bdmpp)(dc\text{-}bpy)(NCS)](PF_6)$ (Ru-NCS) | 1602 (s), 1535 (s), 1471 (s), 1370 (w), 1267 (s), 1022 (s), 792 (s), 695 (w), 639 (s), 508 (s), 382 (s), 141 (vvs) |
| $Ru(iph\text{-}terpy)(phpa\text{-}terpy)Cl_2$ (Ru-terpy) | 1595 (vs), 1554 (s), 1523 (vs), 1466 (vs), 1350 (vs), 1289 (s), 1250 (s), 1157 (s), 1086 (s), 1042 (s), 1016 (s), 831 (s), 667-679 (s), 513 (s), 448 (w), 393 (s), 317 (s), 145 (vvs) |

s: Strong, vs: very strong, vvs: very very strong, w: weak, vw: very week, and vvw: very very week.

ent dyes in 0.1 M KI + $10^{-3}$ M $HClO_4$ aqueous solution. In all cases and independently of the dye, the main effect of the presence of electrolyte is the appearance of two new bands in the range of low wave numbers, centered at 112 and 167 $cm^{-1}$ respectively. The bands intensity is very strong and indeed comparable with that of the main vibration peak of the titania substrate ($E_g$ anatase band at 143 $cm^{-1}$). In this domain (below 200 $cm^{-1}$) no dye bands are expected. Some changes were also observed on the nature of the Raman vibration bands of the pyridine ligands (frequency shifts and intensity variation), which proves that their electronic structure is affected. Thus, besides an important deformation in the high wave number domain, we note the existence of an additional weak peak (shoulder) at 1585 $cm^{-1}$, well distinguished from the 1600 $cm^{-1}$ vibration band. This peak will be better separated under applied potential (see next paragraph).

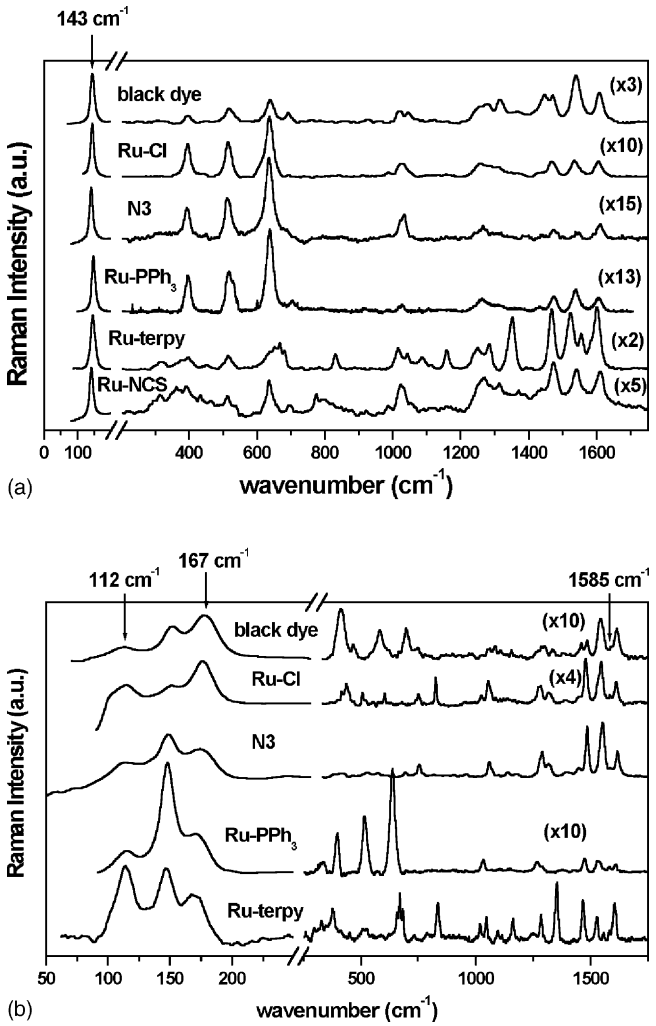


Fig. 1. RR Spectra of dye-sensitized $TiO_2$ electrodes without electrolyte (a) under open-circuit conditions in 0.1 M KI + $10^{-3}$ M $HClO_4$ aqueous solution (b). Magnification concerns the spectrum range above 250 $cm^{-1}$.

### 4.2. Polarization effects

It is generally approved that photon-assisted charge transfer processes can be modulated by the potential applied to the electrode, i.e. the charge transfer process is resonantly excited when the applied potential and the laser excitation energy can promote the electron (or hole transfer) process from a local density of donor states near the Fermi level to the acceptor LUMO (or donor-HOMO) states of the adsorbate [23]. On the other hand, it has been demonstrated that the vibration modes of different dye ligands are dependent on the applied bias and can be selectively enhanced by altering the electrode potential [10,20]. The purpose of using the three-electrode configuration is to discriminate different potential ranges (i.e. the direct current regime, the recombination region and the photocurrent plateau) as a function of the reaction kinetics. Thus, the introduction of the reference electrode inside the cell permits a dynamic control of the photoelectrode/electrolyte interface (no interference from species or reactions taking place at the counter electrode), together with a tracing of the corresponding cell current. In this direction, it is interesting to see in details how the value and sign of the applied potential might influence the behavior of the Raman spectra and especially the appearance, intensity and frequency of the new vibration bands, observed at 112, 167 and 1585 $cm^{-1}$, respectively.

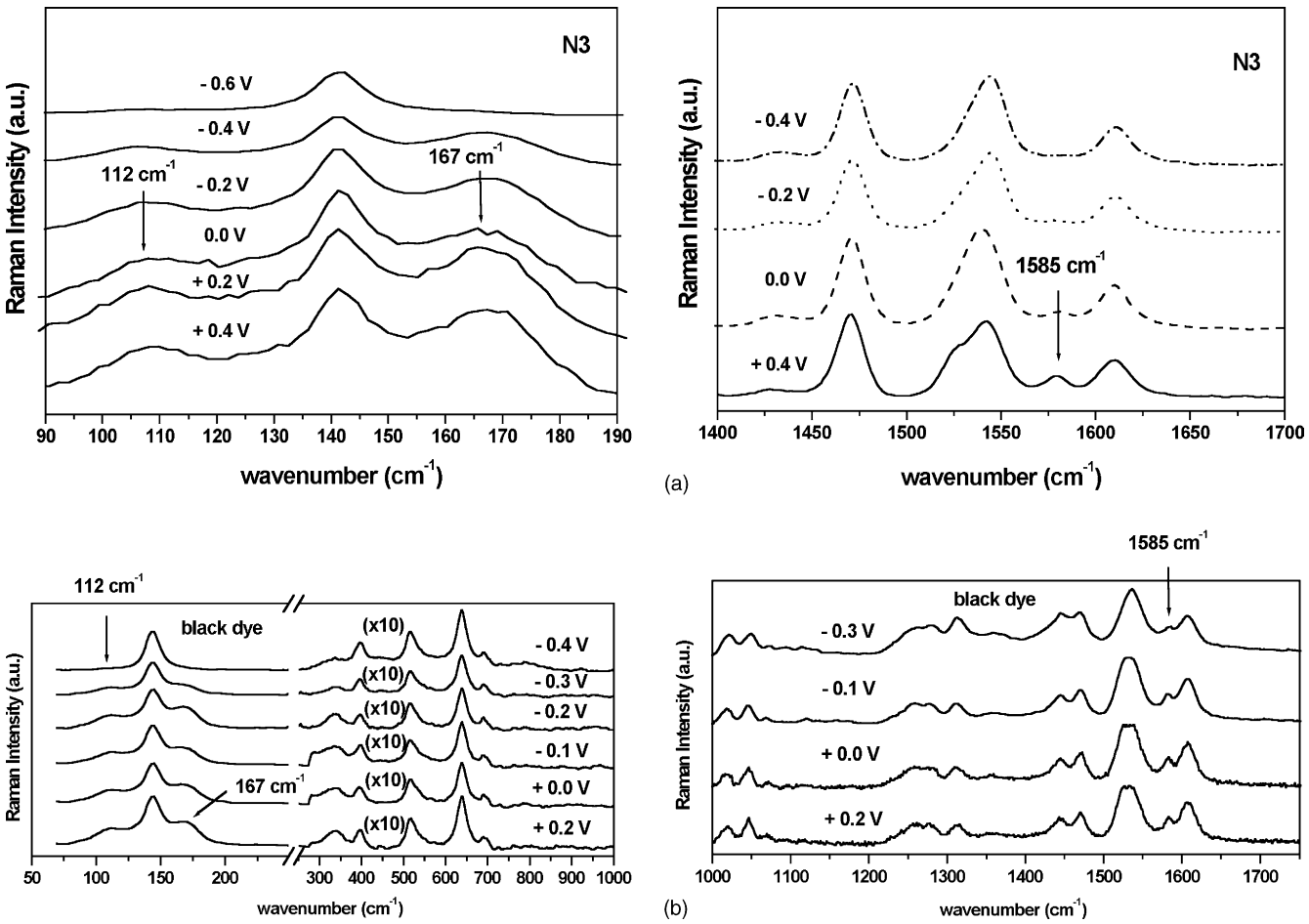


Fig. 2. RR spectra of dye-sensitized $TiO_2$ electrodes polarized in 0.1 M KI + $10^{-3}$ M $HClO_4$ aqueous solution: low wave number range (left) pyridine ring vibrations (right) N3 (a) black dye (b).

The Raman spectra of the nanocrystalline titania electrodes sensitized with four different dyes (N3, black dye, Ru-$PPh_3$ and Ru-terpy) polarized in a three electrode electrochemical cell containing 0.1 M KI + $10^{-3}$ M $HClO_4$ aqueous solution (Ref: SCE, CE: Pt), are given in Figs. 2 and 3. Very interesting phenomena were observed in the lower part of the Raman spectra (wave numbers below 200 $cm^{-1}$). In fact, the two new "satellite" peaks centered respectively at 112 and 167 $cm^{-1}$ are generally present. The stability and reversibility of these bands were checked by performing a series of Raman experiments with consecutive steps of 0.1 V in both the anodic and cathodic range, at increasing and decreasing potentials. The use of different laser lines: red (632.8 nm), green (514.5 nm) and blue (488 nm) does not induce changes in the frequency of the new Raman bands. However, in this case different resonant profiles were observed. The 112 $cm^{-1}$ vibration is enhanced in the blue. This means that the origin of the bands is not the same. In addition, it appears that the lower satellite is very stable; the 112 $cm^{-1}$ band is affected only at very cathodic potentials and disappears at about −0.9 V versus SCE, Fig. 3a. On the contrary, the higher satellite (the 167 $cm^{-1}$ band) is stable only in conditions of photocurrent generation.

The 1585 $cm^{-1}$ Raman vibration peak (shoulder) seems to emerge from (and against) the 1600 $cm^{-1}$ main vibration group and has a behavior similar to that of the 167 $cm^{-1}$ band: it is well distinguished at potentials more positive than −0.3 V approximately and its intensity slightly increases with the increase of the applied bias. In parallel, the relative intensities of the vibrations in the 1400–1600 $cm^{-1}$ range are seriously affected. Their intensity generally increases, when the polarization potential decreases and this is the sign of a severe deformation of the pyridine network. Besides the excellent reversibility of the whole process, it must be stressed that the presence and intensity of these supplementary bands can be easily controlled by properly tuning the applied potential.

### 4.2.1. Influence of the dye

In the aqueous solution containing 0.1 M KI + $10^{-3}$ M $HClO_4$, the same behavior concerning the three new peaks was observed with the totality of the six dyes tested. It was thus confirmed that the presence, appearance or disappearance and potential dependence of the 112, 167, and 1585 $cm^{-1}$ bands and therefore their general conduct do not depend on the nature of the dye selected. However, it must be

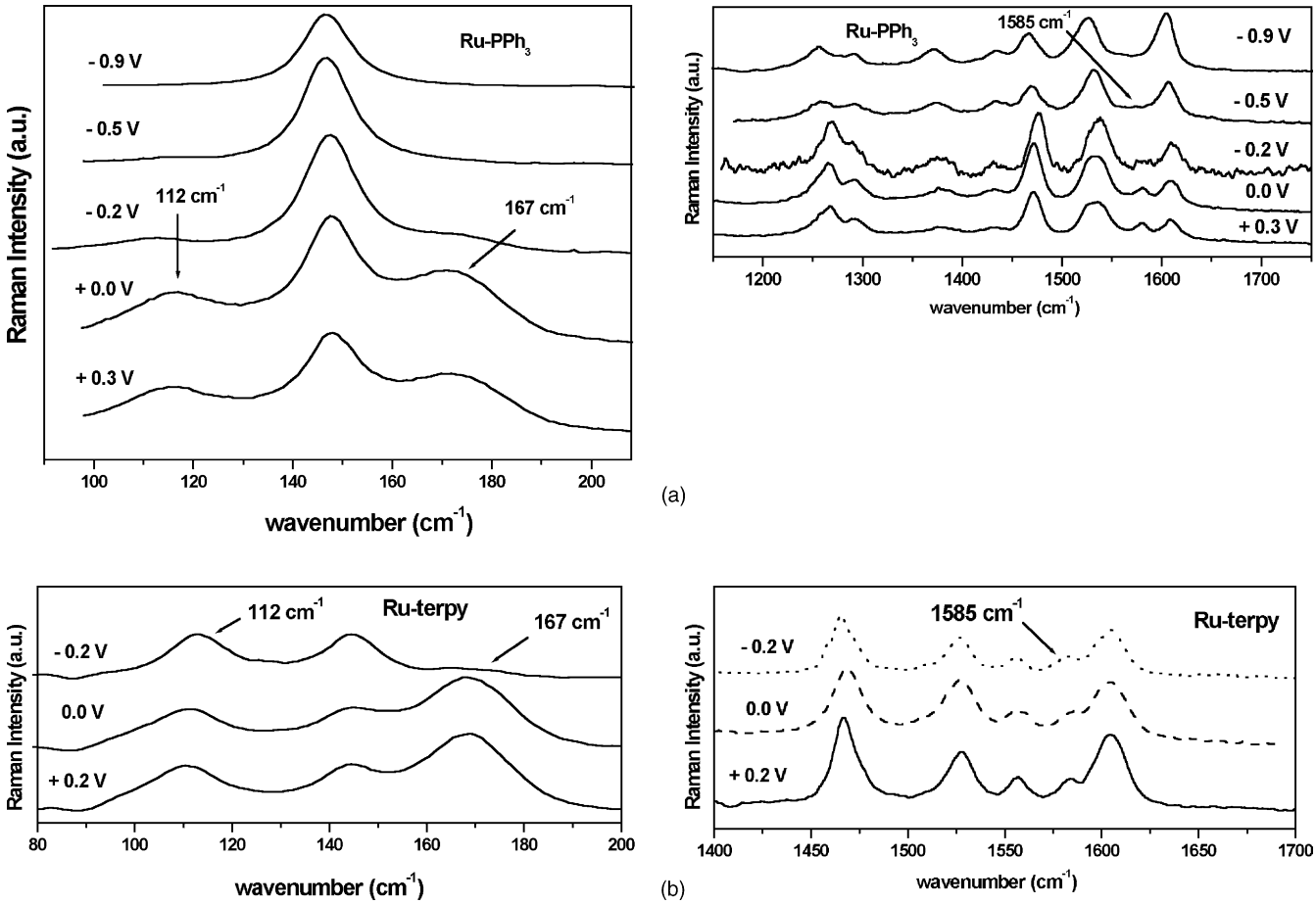


Fig. 3. RR spectra of dye-sensitized $TiO_2$ electrodes polarized in 0.1 M KI + $10^{-3}$ M $HClO_4$ aqueous solution: low wave number range (left) pyridine ring vibrations (right) Ru-$PPh_3$ (a) Ru-terpy (b).

mentioned that no additional peak existed when Pyrogallol Red (a non-pyridyl bearing dye) was used as the sensitizer [11], although normal cell operation and high photocurrents were obtained. The six dyes are characterized by a judicious combination of different ligands (mainly polypyridine). As a consequence, in any case the new Raman peaks can be at least related to bpy or terpy ligands. On the contrary, it must be noticed that the dyes are chemically adsorbed on $TiO_2$ via an ester-like linkage formed between the functional groups of the polypyridine ligands and the hydroxyl moieties (–OH) present on the semiconductor surface [22]. The three new bands are not differentiated with the use of dyes bearing different interlocking agents (−COOH, $-PO_3H_2$). This excludes the possibility of direct or indirect contribution from the functional anchoring groups of the dye. On the other hand, the fact that a very similar behavior was observed with dyes endowed with and mainly with dyes not having $NCS^-$ ligands (Fig. 3a and b) as well as even with dyes of comparable molecular structure indicates that no one of these bands can be associated with the presence of thiocyanate ligands on the sensitizer. Moreover, it is very important to clarify if these supplementary Raman bands are or not related to the presence of the dye. Fig. 4a shows the corresponding Raman spectra of the non-sensitized titania electrode in the aqueous electrolyte (0.1 M KI + $10^{-3}$ M $HClO_4$), under polarization. The major difference is the characteristic absence of the 167 and 1585 $cm^{-1}$ (not shown) Raman peaks, which indicates that the above peaks exist only in the presence of the dye. On the contrary, the 112 $cm^{-1}$ band is always present and slightly increases with the cathodic potential.

*4.2.2. The semiconductor substrate*

To eliminate the possibility of the influence of the semiconductor nature or the preparation method on the observed phenomena, we used three different types of porous nanocrystalline $TiO_2$ electrodes: titanium dioxide Degussa P25 (previous study, 70% anatase-30% rutile), commercial $TiO_2$ paste from Solaronix (Ti–Nanoxide T, 100% anatase) and also $TiO_2$ sol–gel thin films [21]. No supplementary peaks (besides those at 112, 167 and 1585 $cm^{-1}$) were observed and the results were perfectly reproduced in terms of frequency and potential dependence of the three new bands. It is then clear that the presence and behavior of the above peaks does not depend on the preparation method of the titania thin film electrode. Furthermore, it is important to notice that the choice of the semiconductor does not modify

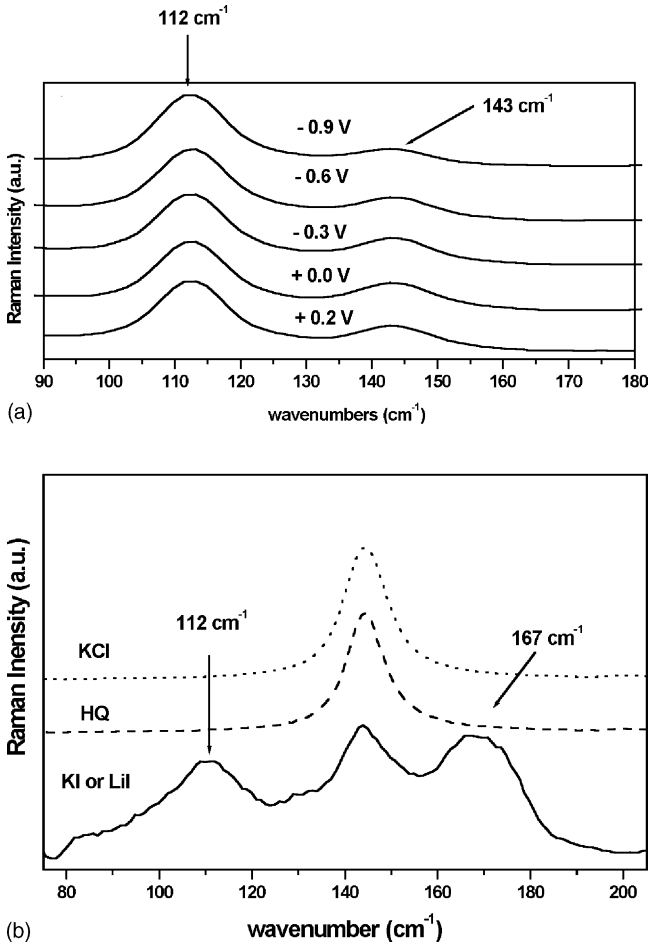


Fig. 4. Raman spectra of $TiO_2$ electrode (without dye) polarized in 0.1 M KI + $10^{-3}$ M $HClO_4$ aqueous solution (a) Raman spectra N3/$TiO_2$ photoelectrode in $10^{-3}$ M $HClO_4$ aqueous solutions of KI or LiI, hydroquinone (HQ), and KCl (b).

the above behavior. In fact, very recent studies realized on solar cells using dye-sensitized tin oxide ($SnO_2$) electrodes confirmed the presence and potential dependence of the additional vibration bands [24].

#### *4.2.3. The role of the electron donor: dye–redox couple interaction*

The role of the redox couple in a dye-sensitized solar cell is preponderant. The iodide ions function to reduce the oxidized dye after electron injection and then they transport the "hole" to the cathode. In the recombination region, the first reaction practically does not take place as Ru(III) recombines with the photoinjected electron. The intensity of the new Raman spectral features depends on the electron donor amount in the KI aqueous solution, and increases by increasing the iodide concentration from 0.01 to 1 M [10]. On the other hand, the above analysis confirms without any doubt that the 167 and 1585 $cm^{-1}$ peaks can be associated with the dye, whereas the 112 $cm^{-1}$ peak is linked to the electrolyte. The direct involvement of the iodide anions was proved when the electron donor KI was replaced by KCl, a simple salt and non-redox active electrolyte. In that case (without any electron donor) it was impossible to detect a photocurrent, no supplementary vibration bands were observed and the obtained Raman spectra, Fig. 4b, were very similar to those obtained ex situ on the modified dye/$TiO_2$ electrodes.

Furthermore, when hydroquinone (HQ) is used at the place of KI as the electron donor in a perchloric acid solution, while the recording of photocurrent shows that the sensitization mechanism is functioning and that the electrode photocurrent is in phase with the laser illumination, the three bands are completely absent and no additional feature become visible in the whole Raman spectrum. In the contrary, when 0.1 M LiI replaced KI, the three Raman bands were present and their behavior did not change. The addition of iodine ($I_2$) in the KI or the LiI electrolyte does not dramatically change the above behavior. In this case, the same additional peaks appear with enhanced intensities. In conclusion, the new bands appearance seems to be in direct relation with the presence of the electron donor and especially the iodide/triodide species in the electrolyte. The first one (112 $cm^{-1}$) is independent on the dye but the other two (167 and 1585 $cm^{-1}$) involve the presence of both the dye and iodide–triiodide and probably their interaction. Furthermore, although the bands are associated with the presence of the iodide, the frequency of the additional Raman features does not depend on the iodide concentration.

## 5. Resonance Raman in real cells

### *5.1. Investigation in organic medium*

The nature of the electrolyte (liquid, semi-solid, solid) strongly affects the ionic mobility and conductivity and has a strong influence on the overall cell's efficiency (photocurrent and photovoltage), stability and lifetime. In the case of the aqueous electrolyte our results demonstrated that the formation of the new Raman bands is drastically correlated to the presence of iodide/triodide species present at the dye/electrolyte interface. It presents big interest to check if they are dependent (or independent) on the nature of electrolyte: aqueous or organic, liquid or solid. On the other hand in order to improve and optimize the performance of the dye-sensitized solar cells it is very important to confirm our results in real cells. Thus, the Raman experiments were performed in cells using an organic solvent—propylene carbonate (PC) containing the $I^-/I_3^-$ (0.1 M LiI + 0.01 M $I_2$) redox couple. The counter-electrode is a $SnO_2$ transparent conductive glass onto which a very small platinum layer is deposited to give a catalytic effect and lower the electron donor reduction overpotential. The electrolyte is introduced between the two electrodes. A spacer (thickness about 50 μm) is placed between the two electrodes to avoid short-circuiting and ensure the thickness of the electrolyte. The studied system is therefore: $SnO_2$:F/$TiO_2$ + dye/PC + 0.1 M LiI + 0.01 M $I_2$/Pt/$SnO_2$:F.

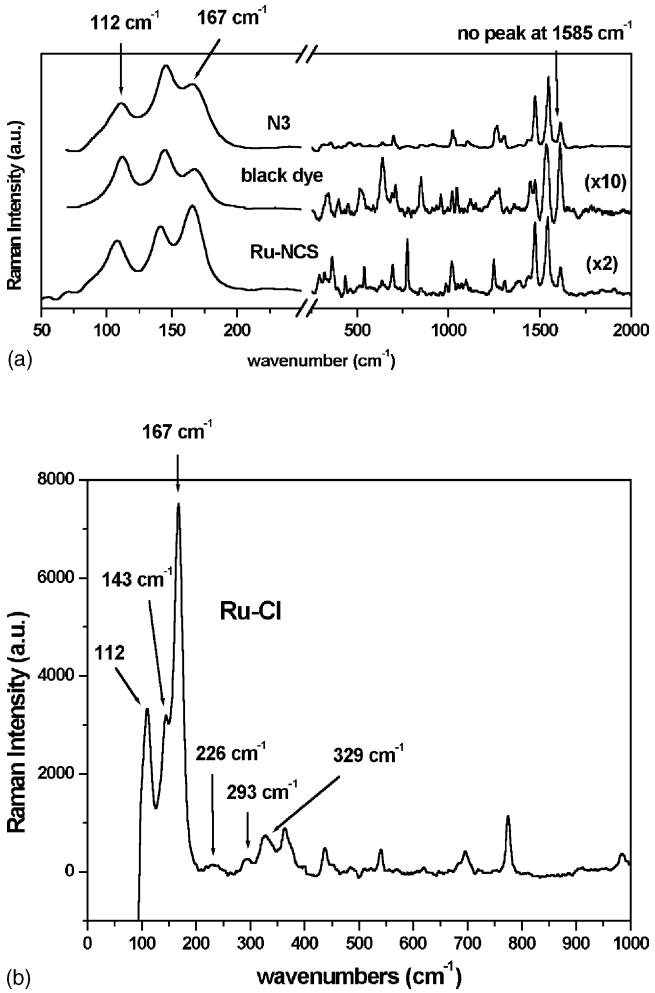


Fig. 5. RR spectra of $TiO_2$ solar cells sensitized with N3, black dye, and Ru-NCS dyes under open circuit potential (ocp) conditions using 0.1 M LiI + 0.01 M $I_2$ + propylene carbonate (PC) organic electrolyte (a) the corresponding spectra obtained with the Ru-Cl dye in the low wave number range, showing the first overtones of the new peaks (b).

Fig. 5a presents the recorded Raman spectra under open circuit conditions for three different dyes: N3, black-dye, and Ru-NCS. In the low wave number range, the new "satellite" vibration bands at 112 and 167 $cm^{-1}$ are still present.

In addition, a more careful analysis for the Ru-Cl dye shows the first overtones (of weak intensity) of these bands, which appear also, at ~221, and 330 $cm^{-1}$, Fig. 5b.

The corresponding overtone of the 143 $cm^{-1}$ anatase vibration appears also at 293 $cm^{-1}$. In the range of pyridine vibrations, the main difference is the complete absence of the 1585 $cm^{-1}$ band. Besides some additional features coming from the solvent (propylene carbonate), other noticeable differences were not observed.

Anodic or cathodic cell polarization does not affect the vibration frequencies of the new bands, Fig. 6. The relative peak intensity in the aromatic and azo-aromatic domain depends on the applied bias. As an example, a reversible behavior of the band at 1540 $cm^{-1}$ was observed, as its intensity increases by increasing the cathodic potential and decreases in the anodic domain [12]. The most important features were observed in the wave numbers range below 200 $cm^{-1}$. For the black dye, Fig. 6b, the intensity of the 112 $cm^{-1}$ band is independent on the anodic potential but strongly dependent on the cathodic potential. It starts to decrease when the potential is below −0.3 V. In the photocurrent plateau range, the intensity of 167 $cm^{-1}$ band increases and seems to reach a max between 0.2 and +0.3 V. When the potential decreases, the peak at 167 $cm^{-1}$ progressively diminishes and disappears first, at about −0.3 V.

The intensity of both bands depends on LiI (iodine) content in the electrolyte and considerably increases with the increase of the electrolyte concentration, as it is shown in Fig. 7 for a cell using the N3 dye. The same phenomenon was observed with a number of other dyes and the presence of the two satellite peaks is drastically correlated to the existence of species at the dye–electrolyte interface originating from reactions between the dye and the redox couple.

### 5.2. Study in a solid-state electrolyte

In order to overcome solvent evaporation and sealing problems encountered with liquid electrolytes, which directly affect their stability and long-term operation, many efforts have been made to develop photoelectrochemical cells using solid matrices containing the iodide–triiodide redox couple. Recently, we reported on the assembling of solid-state dye-sensitized solar cells using a polymer composite electrolyte with an inorganic oxide as the filler, in the presence of the $I^-/I_3^-$ redox couple [25]. In this study, we also used in situ resonance Raman spectroscopy to get information about the photoelectrode/solid electrolyte interface.

The new solvent-free composite polymer electrolyte consists of high-molecular mass poly(ethylene) oxide (PEO) filled with titanium oxide ($TiO_2$ Degussa P25) and containing LiI and $I_2$. The polymer chains separated by the titania particles are arranged in a three-dimensional, mechanically stable network, that creates free space and voids into which the iodide/triodide anions can easily migrate. The dye-modified electrodes were incorporated in a solid-state dye-sensitized solar cell using the composite electrolyte. A series of Raman spectra obtained with cells using the N3 and Ru-Cl dyes under polarization, is shown in Fig. 8. The two strong satellites in the low wave number range, at 112 and 167 $cm^{-1}$ respectively, are still present.

The 167 $cm^{-1}$ vibration band is very sensitive to the applied potential. Its intensity progressively decreases and disappears at −0.9 V. The other band centered at 112 $cm^{-1}$ seems to be less sensitive as it considerably decreases only at very low negative potentials, at about −0.9 V. It is worth mentioning that the relative bands intensity seems to depend on the dye selected. On the other hand, looking at the 1300–1600 $cm^{-1}$ range, one could observe a net deformation, which consists of a decrease of the pyridine bands intensity under anodic bias. However, the 1585 $cm^{-1}$ peak is

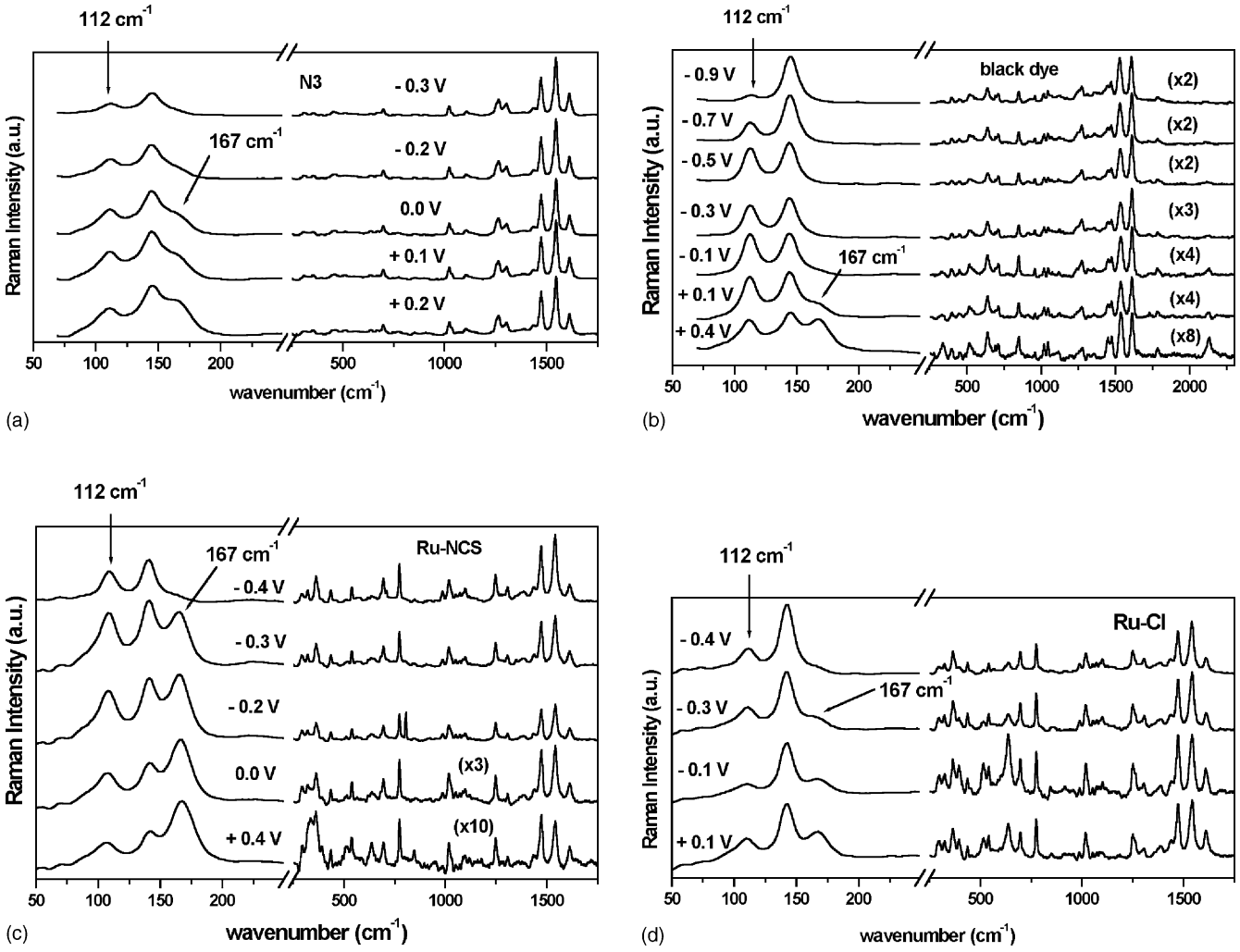


Fig. 6. RR spectra of dye sensitized $TiO_2$ solar cells using 0.1 M LiI + 0.01 M $I_2$ + propylene carbonate (PC) organic electrolyte under polarization: N3 (a) black dye (b) Ru-NCS (c) Ru-Cl (d).

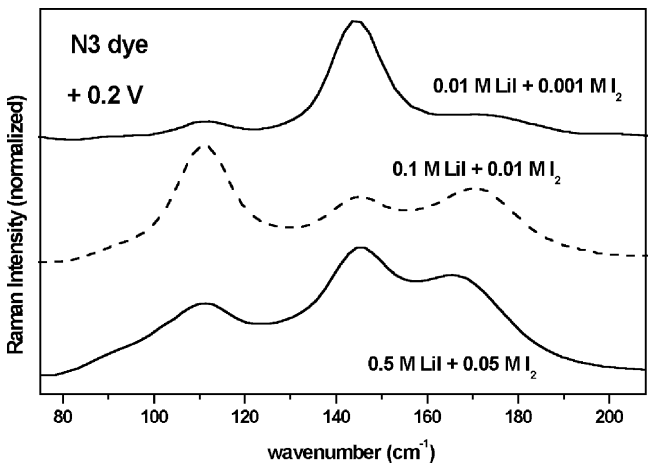


Fig. 7. RR spectra of $TiO_2$ solar cells sensitized with N3 dye polarized at +0.2 V in LiI + $I_2$ + propylene carbonate (PC) organic electrolyte as a function of the redox couple concentration.

absent and cannot be observed with any dye. In conclusion, one could postulate that in general the Raman behaviour is independent on the cell's configuration, liquid, or solid.

## 6. Attribution of the new Raman peaks

Some other groups have also attempted to investigate the vibrational properties of the dye and the sensitized electrode–electrolyte interface. To explain the degradation phenomena that limit the stability and lifetime of the cell, a mechanism of thiocyanato ligand exchange has been proposed [14]. By resonance Raman scattering they observed a weak supplementary vibration line at 165 $cm^{-1}$ and attributed it to a ligand exchange reaction involving the formation of a complex ($I_2SCN^-$) between the thiocyanato ligands ($SCN^-$) and iodine ($I_2$). However, very recently, they concluded that $I_2SCN^-$ is formed only to a small extend and that triiodide was found to exchange the $SCN^-$ of the dye [15]. Lavrencic Stangar et al. [16] recorded

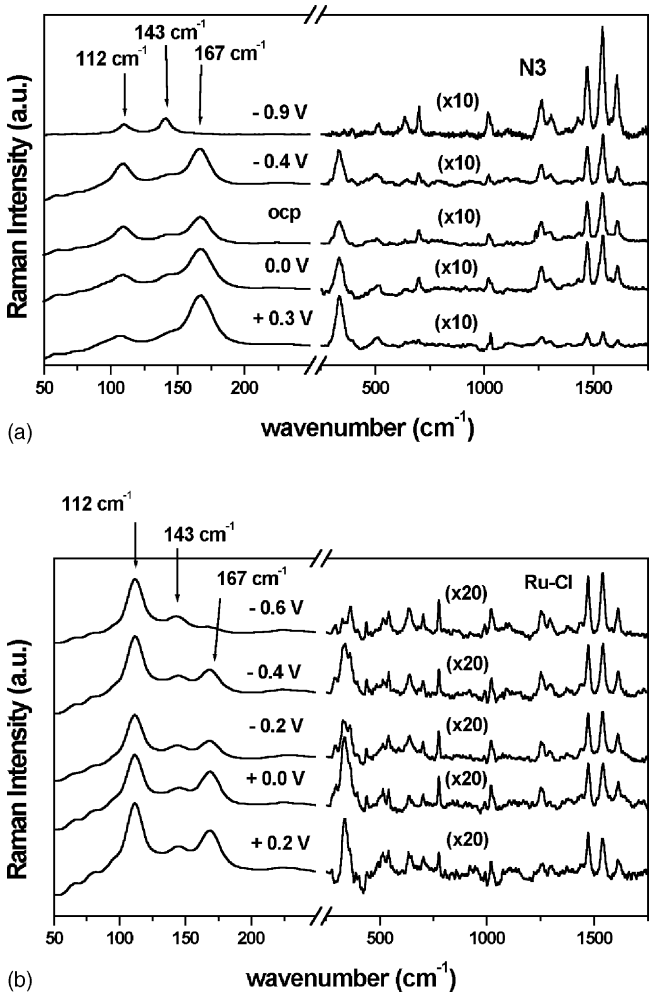


Fig. 8. RR spectra of solid-state $TiO_2$ solar cells under polarization: N3 dye (a) Ru-Cl dye (b).

the resonance Raman spectra in a DSC using a sol–gel (solid) electrolyte containing the $I^-/I_3^-$ redox couple, which was based on organosilane consisting of chemically bonded poly(ethylene glycol) to triethoxysilane endcapping groups. They observed RR bands at 111 and 166 $cm^{-1}$ and attributed them to the formation of $I_3^-$ species and iodine–solid–electrolyte complex respectively. The assignment of the 166 $cm^{-1}$ band to the symmetric stretching of the iodine-ICS–PPG complex [$\nu_1$(I–I)$_{ICS-PPG}$] is not well supported and seems to be arbitrary. It must be pointed out that both papers were mainly centered on the cell stability and the understanding of degradation mechanisms that limit the lifetime of the cell. Although the dependence of the Raman spectra on the polarization was unambiguously established, the authors studied the DSSC at open circuit (ocp) and short circuit (sc) conditions only. They both used the same dye (N719 or N3) containing the thiocyanate ligand ($NCS^-$) under conditions that are far from being ideal: in hostile electrolytes where important degradation occurs or where the long-term operation of the cell is problematic.

The detailed investigation of the 112 and 167 $cm^{-1}$ bands under polarization in both aqueous and non-aqueous media has shown that these bands have different resonance profiles. Therefore, they can not originate from the same species. The lower wave number band (112 $cm^{-1}$) was well identified in charge transfer complexes as in solid compounds [11,14,16,31,32] and can be unambiguously assigned to the $\nu_1$ symmetric stretching vibration of the $I_3^-$ moiety. On the contrary, the proposed assignment of the 167 $cm^{-1}$ band to the formation of a complex between triiodide and thiocyanate ligand cannot be accepted, as it appears also with dyes which do not have SCN ligands. In addition, its attribution to an $I_2$–solid electrolyte complex must be excluded, as the band was observed in a number of different electrolytes, both liquid and solid.

The correct assignment of the 167 $cm^{-1}$ satellite in photo–electrochemical systems was not given up to now, probably because the universal character of this band was not enough taken into account. The simultaneous presence of $I^-$ and $I_2$ moieties in the electrolyte gives rise to the formation of polyiodide anions such as $I_3^-$ and $I_5^-$ [33]. The presence of the 167 $cm^{-1}$ band in the region (100–200 $cm^{-1}$) where the Raman active modes of polyiodides are found in literature, indicates that this band is probably related to the I–I vibration. A similar band was observed in the iodine–pyridine charge transfer complexes in solution and assigned to an intermolecular vibration involving iodine and dye [26]. Working on a large number of polyiodides and neutral $I_2$-adducts with donors, Deplano et al. [27] have shown that these adducts are associated with the appearance of the $\nu_{I-I}$ vibrations in the 140–180 $cm^{-1}$ range . Following this description, the $I_3^-$ ion can exist as a real entity (bond order ~0.5, symmetrical I–I–I stretching at 110 $cm^{-1}$) or as an $I^-$. $I_2$ adduct (for a 0.8 $I_2$ bond order a peak at 167 $cm^{-1}$ assigned to I–I stretching is observed. A band around 167 $cm^{-1}$ was also detected in a large number of pentaiodide complexes, containing $I_5^-$ in a linear configuration [28–30].

The dye regeneration occurs following interaction with iodide

$$2D^+ + 3I^- \rightarrow 2D + I_3^- \quad (1)$$

and then $I_3^-$ travel to the counter electrode to catch an electron and get reduced back. In parallel, the formation of an intermediate complex involving an electrostatic binding of $D^+$ with $I_3^-$ is possible

$$D^+ + I_3^- \rightarrow [D^+]I_3^- \quad (2)$$

In this case, the triiodide is attached to the whole complex by electrostatic (coulomb) forces. Therefore, modifications resulting in the stretching mode of the iodine would be detectable in Raman. But what kind of electrostatic attachment can occur between the dye and the polyiodides?

Recently, a series of $[Cr(III)(L)_2(NCS)_2]X$ complexes, where L is 2,2′-bipyrine (bpy) or 4,4′-dimethyl-2,2′-bipyrine

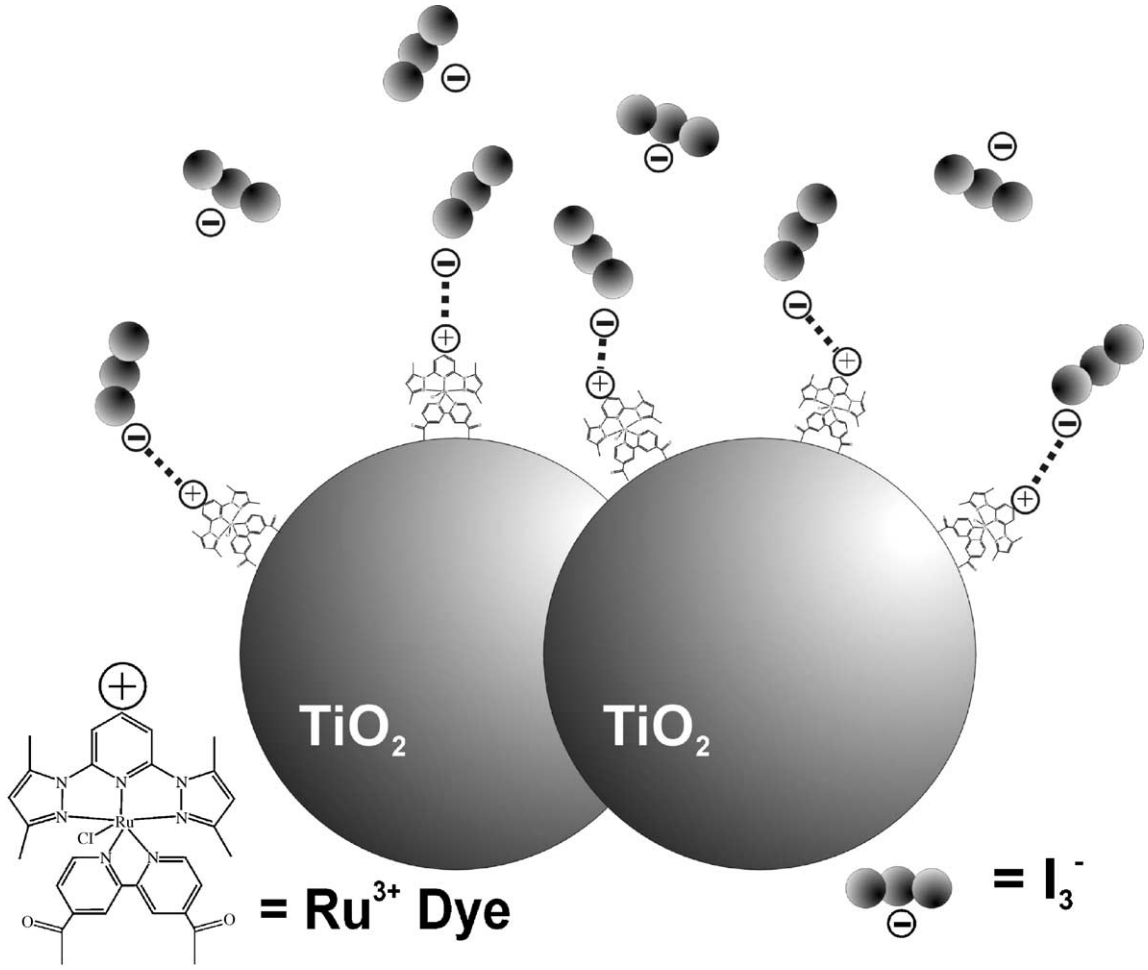


Fig. 9. Proposed model for the formation of $[D^+]I_3^-$ complex showing electrostatic binding between the oxidized form of the dye ($Ru^{3+}$) and triiodide ($I_3^-$).

(dmp) and $X^-$ is $I^-$, $I_3^-$ have been prepared for study as surrogates for photo-oxidized "$N3^+$" dye [34]. X-ray structural determination of the above bpy complex as the $I_3^-$ salt, indicated a charge transfer interaction between the one of the bpy ligands and one of the terminal iodine atoms of the anion. Following these authors such an interaction potentially could be involved in the unique function of the $I^-/I_3^-$ couple in the cell. The $I_3^-$ anion sits near and above the plane of the pyridine ligands. The closest carbon atom of the bpy ring sits 3.711 Å from the terminal iodine ions. Milne [35] studied the HI–$I_2$ system in aqueous solutions and observed extra spectral features at about 172 $cm^{-1}$. They attributed it to the I–I stretch of the $[H^+]I_3^-$ ion-pairs. A similar band at 170 $cm^{-1}$ was observed in different solutions of triiodides with $R_3S^+$ cations and assigned to the $I_2$ $\upsilon_1$ mode [36,37].

The presence of the 167 $cm^{-1}$ vibration band gives a clear indication of a significant charge transfer from the $I_3^-$ into the nearest pyridine moiety and may correspond to a similar charge transfer interaction during the formation of a $I_3^-$–Ru(III) complex. In fact, the pyridine rings chelated to the metal have poor π-electron density since the N atom (Ru-bonded) disposes a positive charge that attracts the electrons of the ring. Since the dye is positively charged ($D^+$) the electron density of the pyridine ring is even smaller this time. Then, polyiodides can easily offer their electrons to the pyridine ring forming a charge transfer complex, Fig. 9.

The use of the Raman microscope gives us the possibility of the spatial resolution–distribution of the new species. The results show that these species created during the cell operation are mainly localized on the photoelectrode and not on the counter electrode. Moreover, the performances of confocality permitted the study of species distribution on the photoelectrode. By focusing the laser either on the inner part of the interface ($TiO_2$ side) or on the outer part (electrolyte side), the difference in the 112 and 167 $cm^{-1}$ band intensities shows that the DI is inner and covered by triiodide on the electrolyte side [11]. The proposed model is in excellent agreement with the observed behavior of the 167 $cm^{-1}$ band in the recombination and direct current ranges. That is, at negative potentials, the disappearance of the 167 $cm^{-1}$ band is due to the non-availability of the $D^+$ species to form the $[D^+]I_3^-$ complex. On the contrary, when the electrode is positively polarized we assist on the increase of the peak at 165 $cm^{-1}$, as the $D^+$ species production is enhanced. Ad-

ditionally, positive charging of the electrode surface attracts any anionic species ($I_3^-$) at the interface dye–electrolyte. Hence the formation of $[D^+]I_3^-$ pairs increases.

The observed potential dependence of the intensity of the 1400–1600 $cm^{-1}$ range (increase in the cathodic and decrease in the anodic domain), as well as the appearance and behavior of the 1585 $cm^{-1}$ band in the aqueous electrolyte (very similar to that of the 167 $cm^{-1}$) clearly support the proposed formation of $[D^+]I_3^-$ complex. In fact, such an interaction would influence not only the triiodide vibration Raman bands (167 $cm^{-1}$) but also the pyridine ones. Taking into account the ionic character of these intermediates, it is expected that the $[D^+]I_3^-$ species are better stabilized in an acidic medium than in the organic solvent [35]. Therefore, the 1585 $cm^{-1}$ peak corresponds to a deformation vibration of the $\omega_7$ C-C stretching vibration, usually present at 1600 $cm^{-1}$ in the original dye molecule. Such a deformation may result from the adjacency and direct interaction between the dye pyridines and the $I_3^-$ species.

## 7. Conclusions

Rough, high surface area nanocrystalline $TiO_2$ films were successfully sensitized by light harvesting molecular antennas consisting of Ru(II) complexes with bpy, terpy and bdmpp ligands, bearing functional anchoring groups ($-COOH$, $-PO_3H_2$). In situ characterization of the dye–electrolyte interface by resonance Raman spectroscopy confirmed the presence of new species resulting from the triiodide species and more important, from a direct interaction between the dye and the $I^-$–$I_3^-$ redox couple.

New Raman bands were observed at 112 and 167 $cm^{-1}$ in the low wave number region, together with a deformation of the pyridine framework. An additional vibration appears also at 1585 $cm^{-1}$ in acidic aqueous electrolytes. The phenomenon is common to all dyes containing azoaromatic ligands (mainly bpy and/or terpy). The presence of the peaks does not depend neither on the preparation and nature of the semiconductor, but there are related to the simultaneous presence of iodide in the electrolyte and pyridine (azo-aromatic) moieties on the dye ligands. The 112 $cm^{-1}$ band is relatively stable in the photocurrent plateau and the recombination range. It disappears only at very cathodic polarization. The band is assigned to the $\nu_1$ vibration of the $I_3^-$ moiety. The 167 $cm^{-1}$ vibration band appears in conditions of photocurrent generation and its intensity is strongly dependent on the potential. It is stable in the photocurrent plateau and disappears in the cathodic range. The same phenomenon was observed in a large number of different dyes bearing bipyridine or/and terpyridine ligands, in presence of triiodides. The band is associated to the oxidized state, $D^+$, of the dye and is assigned to the symmetric stretching vibration $\nu$(I–I) of the triiodide in the chemically stable $[D^+]I_3^-$ complex and is compatible with a consequent increase in the I–I distance. The 1585 $cm^{-1}$ band is attributed to a deformation of the $\omega_7$ (or $\upsilon_5$) C–C stretching vibration of the pyridine group, stabilized in the acidic medium. This stabilization, not possible in the organic medium (exempt of protons), produces a lowered bond order within the pyridine group and is reflected by the lowered frequency. Recently, both micro- and macro-Raman (in that case the laser power density upon the photoelectrode is severely reduced) experiments were performed on DSSC devices under variable forward and reverse bias. Armonic osscilation modeling and Lorenzian fitting on the Raman data seem to confirm the behavior of the 167 $cm^{-1}$ peak in terms of frequency and intensity dependence from the applied bias [38].

## Acknowledgements

Thanks must be addressed to Prof. V.J. Catalano, Prof. I. Lukes, Dr. M. Kalbac, Dr. A.P. Xagas, Dr. A. Chryssou, I.M. Arabatzis for valuable assistance and to Degussa AG Frankfurt-Germany for generously supplying the $TiO_2$ P25 powder. Financial support from NCSR Demokritos, France-Greece (Platon) and Germany-Greece bilateral cooperations is also greatly acknowledged.

## References

[1] B. O' Regan, M. Grätzel, Nature 353 (1991) 737.
[2] M.K. Nazeeruddin, A. Kay, I. Rodicio, R. Humphry-Baker, E. Müller, P. Liska, N. Vlachopoulos, M. Grätzel, J. Am. Chem. Soc. 115 (1993) 6382.
[3] K. Kalyanasundaram, M. Grätzel, Coordination Chem. Rev. 77 (1998) 347.
[4] C.J. Barbé, F. Arendse, P. Compte, M. Jirousek, F. Lenzmann, V. Shklover, M. Grätzel, J. Am. Ceram. Soc. 80 (1997) 3157.
[5] N. Papageorgiou, W.F. Maier, M. Grätzel, J. Electrochem. Soc. 144 (1997) 876.
[6] A. Nasr, S. Hotchandani, P.V. Kamat, J. Phys. Chem. 102 (1998) 4944.
[7] A. Rousar, J. Krýsa, K. Bouzek, L. Kavan, Sol. Energy Mat. Sol. Cells 51 (1998) 155.
[8] P. Falaras, M. Grätzel, A. Hugot- Le Goff, M. Nazeeruddin, E. Vrachnou, J. Electrochem. Soc. 140 (1993) L92.
[9] A. Hugot- Le Goff, P. Falaras, J. Electrochem. Soc. 142 (1995) L38.
[10] A. Hugot-Le Goff, S. Joiret, P. Falaras, J. Phys. Chem. B 103 (1999) 9569.
[11] M.C. Bernard, H. Cachet, P. Falaras, A. Hugot-Le Goff, M. Kalbac, I. Lukes, N.T. Oanh, T. Stergiopoulos, I. Arabatzis, J. Electrochem. Soc. 150 (2003) E155.
[12] P. Falaras, K. Chryssou, T. Stergiopoulos, I. Arabatzis, G. Katsaros, V.J. Catalano, R. Kurtaran, A. Hugot-Le Goff, M.C. Bernard, in: Zakya H. Kafafi (Ed.), Proceedings of SPIE 4801 Organic Photovoltaics III, 2003, p. 125.
[13] M.C. Bernard, H. Cachet, P. Falaras, A. Hugot-Le Goff, N.T.T. Oanh, T. Stergiopoulos, in: Zakya H. Kafafi (Ed.), Proceedings of SPIE 4801 Organic Photovoltaics III, 2003, p. 87.
[14] H. Greijer, J. Lindgren, A. Hagfeldt, J. Phys. Chem. B 105 (2001) 6314.
[15] H. Greijer Agrell, J. Lindgren, A. Hagfeldt, Solar Energy 75 (2003) 169.
[16] U. Lavrencic Stangar, B. Orel, A. Surca Vuk, G. Sagon, Ph. Colomban, E. Stathatos, P. Lianos, J. Electrochem. Soc. 149 (2002) E413.

[17] K. Chryssou, V.J. Catalano, R. Kurtaran, P. Falaras, Inorg. Chim. Acta 328 (2002) 204.
[18] K. Chryssou, T. Stergiopoulos, P. Falaras, Polyhedron 21 (2002) 2773.
[19] P. Pechy, F.P. Rotzinger, M.K. Nazeeruddin, O. Kohle, S.M. Zakeeruddin, R. Humphry-Baker, M. Grätzel, J. Chem. Soc. Chem. Commun. 65 (1995) 1093.
[20] P. Falaras, A. Hugot-Le Goff, M.C. Bernard, A. Xagas, Sol. Energy Mat. Sol. Cells 64 (2000) 167.
[21] I.M. Arabatzis, T. Stergiopoulos, G. Katsaros, M.C. Bernard, D. Labou, S.G. Neofytides, P. Falaras, Appl. Catal. B: Environ. 42 (2003) 187.
[22] P. Falaras, Sol. Energy Mat. Sol. Cells 53 (1998) 163.
[23] J. Rubim, P. Corio, M. Ribeiro, M. Manz, J. Phys. Chem. 99 (1995) 15765.
[24] T. Stergiopoulos, M.C. Bernard, A. Hugot-Le Goff, P. Falaras 203rd Meeting of The Electrochemical Society, Paris, France, Paper S1-1675 (April 27–May 2 2003).
[25] T. Stergiopoulos, I.M. Arabatzis, G. Katsaros, P. Falaras, Nano Lett. 2 (2002) 1259.
[26] T. Tassaing, M. Besnard, J. Phys. Chem. A. 101 (1997) 2803.
[27] P. Deplano, J. Ferraro, M.L. Mercuri, E. Trogu, Coordin. Chem. Rev. 188 (1999) 71.
[28] R.C. Teitelbaum, S.L. Ruby, T.J. Marks, J. Am. Chem. Soc. 102 (1978) 3322.
[29] E.M. Nour, L.H. Chen, J. Laane, J. Phys. Chem. 90 (1986) 2841.
[30] A. Sengupta, M. Holtz, E.L. Quitevis, Chem. Phys. Lett. 263 (1996) 25.
[31] G. Maes, J. Mol. Struct. 61 (1980) 95.
[32] R. Wojcicchowski, J. Ulanski, P. Polanowski, S. Lefrant, E. Faulques, Synth. Met. 109 (2000) 301.
[33] W. Kubo, K. Murakoshi, T. Kitamura, S. Yoshida, M. Haruki, K. Hanabusa, H. Shirai, S. Yanagida, J. Phys. Chem. B 105 (2001) 12809.
[34] B.J. Walter, C.M. Eliot, Inorg. Chem. 40 (2001) 5924.
[35] J. Milne, Spectrochim. Acta 46 (1992) 1625.
[36] P.H. Svensson, L. Kloo, J. Chem. Soc. Dalton Trans. (2000) 2449.
[37] M.E. Heyde, L. Rimai, R.G. Kilponen, D. Gill, J. Am. Soc. 94 (1972) 5222.
[38] A.G. Kondos, T. Stergiopoulos, P. Falaras, unpublished results.